DOI 10.1007/s11182-018-1544-x

Russian Physics Journal, Vol. 61, No. 8, December, 2018 (Russian Original No. 8, August, 2018)

PHYSICS OF MAGNETIC PHENOMENA

STUDY OF THE WEAK FIELD SENSOR ON THE RESONANT MICROSTRIP STRUCTURE WITH A THIN FERROMAGNETIC FILM

B. A. Belyaev,[1,2] N. M. Boev,[1,2] A. V. Izotov,[1,2] P. N. Solovyev,[1,2] and V. V. Tyurnev[1,2]

UDC 537.87+517.958

The paper examines the characteristics of the miniature sensor of weak magnetic fields on the resonant microstrip structure with a thin ferromagnetic film. The authors calculated the frequency response of irregular microstrip resonator containing anisotropic magnetic film in quasi-static approximation. The resonator is connected to transmission lines via coupling capacities. The authors determined the optimal directional angles of the constant magnetic displacement field ensuring maximum sensitivity of the sensor. They examined the impact of angular and amplitude dispersion of uniaxial magnetic anisotropy of thin film upon the sensor characteristics. The regularities determined in this research qualitatively agree with the experimental results.

Keywords: microstrip resonator, thin magnetic film, frequency response, sensor of weak magnetic fields, quality factor, scattering matrix, magnetometer.

INTRODUCTION

Design of high-sensitivity sensors of weak magnetic fields is a crucial research and development task. Such devices find wide application in geological prospecting [1, 2], space monitoring [3, 4], and in pursuit of other applied and research tasks [5, 6] that require accurate measurement of magnetic field parameters. One knows numerous technical solutions relying on various physical phenomena that allow creating magnetic field sensors with high threshold sensitivity [7]. SQUID magnetometers [8] and comparable atomic sensors with optical pumping [9, 10] have a record high threshold sensitivity reaching $\sim 10^{-15}$ T. However, such high sensitivity is only reached in highly engineered, large-size and costly units, and SQUID magnetometers also require cryogenic temperatures. That is why one rarely applies such sensors for magnetic measurements in the field conditions, where fluxgate (magnetic modulation) magnetic field sensors are widely used [7, 11]. Their sensitivity is considerably lower than sensitivity of quantum magnetometers and does not normally exceed $\sim 10^{-10}$ T, but these sensors are compact, easy to use and resistant to external impacts. One should note that the upper boundary of the operating frequencies band of fluxgate sensors is only several kilohertz. This is due to the low rate of magnetization reversal of the sensor core, as well as to shielding of measured variable magnetic fields with windings of excitation and detection coils. However, in certain applications, for instance in pulsed electric prospecting with artificial excitation of the medium, one needs magnetometers with an operating frequencies band of at least tens of kilohertz [12].

[1]L. V. Kirensky Institute of Physics of the Krasnoyarsk Research Center of the Siberian Branch of the Russian Academy of Sciences, Krasnoyarsk, Russia, e-mail: belyaev@iph.krasn.ru; iztv@mail.ru; tyurnev@iph.krasn.ru; [2]Siberian Federal University, Krasnoyarsk, Russia, e-mail: nik88@inbox.ru; solap@ya.ru. Translated from Izvestiya Vysshikh Uchebnykh Zavedenii, Fizika, No. 8, pp. 3–10, August, 2018. Original article submitted June 25, 2018.

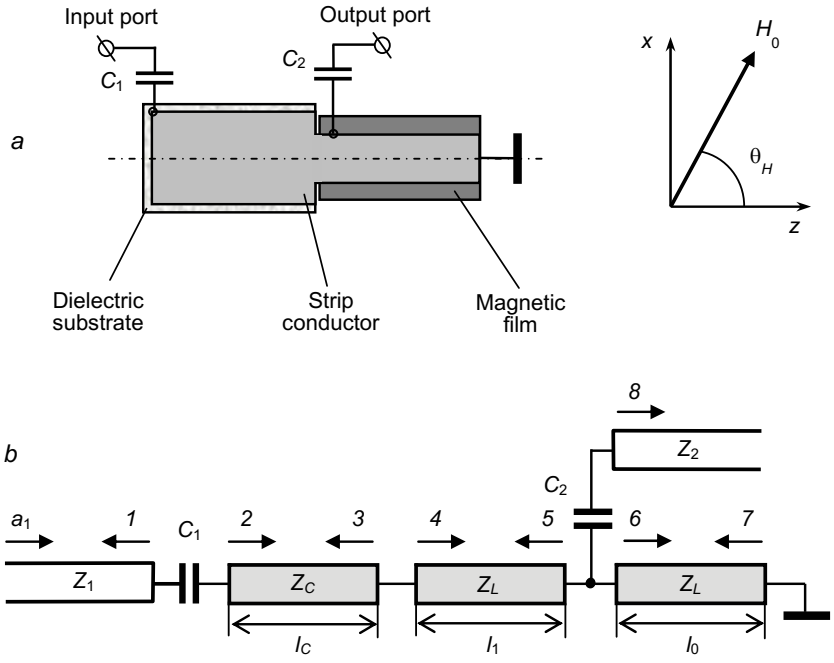

Fig. 1. Design of a sensor on irregular quarter-wave strip resonator with a thin magnetic film (*a*) and its one-dimensional model (*b*).

What holds promise for these applications is a magnetometer of weak quasi-stationary and high-frequency magnetic fields, the sensitive component of which is a thin magnetic film (TMF) possessing uniaxial magnetic anisotropy and placed into a resonant microstrip structure [13]. Thin-film microstrip sensor has a number of advantages compared to other sensors: it is miniature and energy-efficient, but has high sensitivity reaching 10^{-12} T in a wide frequency range of measured magnetic fields (10^{-2}–10^5 Hz).

However, in order to study the possibility of improving the parameters of microstrip sensor developed in [13], one needs to perform mathematical analysis of its physical model. This will enable a theoretical study of behavior regularities of the sensor characteristics when varying parameters of both the microstrip structure and the magnetic film. It is obvious that based on obtained regularities one will be able to optimize the sensor design to achieve the maximum possible characteristics in it.

The authors of the present paper developed a resonant microstrip sensor model based on quasi-static calculation of electromagnetic waves propagating in the planar microstrip line with a thin magnetic film [14]. Numerical analysis of the developed model allows establishing some regularities, for instance behavioral regularities of the sensor conversion factor during the change of value and direction of the constant displacement field.

1. MODEL OF MICROSTRIP SENSOR OF WEAK MAGNETIC FIELDS

The modeled sensor is built on irregular microstrip quarter-wave resonator [13]. This resonator consists of two segments of strip transmission lines (Fig. 1*a*). One of them is wide; it is manufactured on the substrate with high relative dielectric permeability. This segment has low characteristic impedance. One of its ends is free, and another is connected to the second, narrow, segment that has high characteristic impedance. The opposite end of the narrow conductor is circuited to the ground plane. Thin magnetic film is located under the narrow conductor in the antinode of high-frequency magnetic field. The resonator is connected to input and output ports by means of capacitive coupling (Fig. 1*a*).

For calculation, one can present the microstrip structure under consideration as a one-dimensional model (Fig. 1*b*). The model contains segments of microstrip conductors with characteristic impedances Z_C and Z_L ($Z_C < Z_L$), and the microstrip resonator is connected to the input and output ports with characteristic impedances Z_1 and Z_2 via coupling capacities C_1 and C_2. The segment of low-impedance transmission line has the length of strip conductor l_C and its width w_C. The segment of high-impedance strip transmission line has the width w_L and is divided by the output port connection point into two segments with lengths l_1 and l_0. Numbers on the scheme enumerate the amplitudes of incident and reflected waves on the regular resonator segments, as well as on the input and output transmission lines excited by the primary incident wave a_1 on the input port. Arrows indicate the direction of propagation of these waves.

Calculation of the frequency characteristic of the examined microstrip structure will be performed within the one-dimensional model, where the oscillation phase advance occurs only along the strip conductors [15]. Only traveling waves of the main type are explicitly taken into account. Their amplitudes are found by solving the Kirchhoff's equations recorded for all nodal points of the scheme. The impact of higher wave modes localized on irregularities is modeled by introducing effective end capacities. The presence of open-end capacity of the low-impedance line segment is taken into account by effective lengthening of its strip conductor by value Δl that one can calculate using the approximated formula [16]

$$\Delta l = 0.412 h_{\mathrm{d}} \left(\frac{\varepsilon_{\mathrm{re}} + 0.3}{\varepsilon_{\mathrm{re}} - 0.258} \right) \left(\frac{w/h_{\mathrm{d}} + 0.264}{w/h_{\mathrm{d}} + 0.8} \right), \tag{1}$$

where h_{d} is thickness of dielectric substrate of the strip line, w is width of its conductor, $\varepsilon_{\mathrm{re}} = c^2 L_C C_C$ is effective relative dielectric permeability of the substrate (L_C is inductance per unit length, C_C is capacitance per unit length of the microstrip line, c is speed of light).

Let us assume that a unit-capacity wave with circular frequency ω, which normalized amplitude $a_1 = 1$ W$^{1/2}$ corresponds to, falls on the input port of the resonator. On the input port, the voltage amplitude U_1 and the current amplitude I_1 expressed with the following formulas correspond to this normalized amplitude:

$$U_1 = a_1 \sqrt{Z_1}, \quad I_1 = a_1 \big/ \sqrt{Z_1}\,. \tag{2}$$

Secondary incident and reflected waves formed on the boundaries of connection of the regular transmission line segments are propagated in the opposite directions. On any regular transmission line segment one takes into account the phase difference between incident and reflected waves that is determined by electric length of the segment. For instance, for waves *2* and *3* (see Fig. 1) the electric length of the corresponding segment equals $k_C l_C$, where k_C is a wave number. For current amplitudes X_j, where j is the secondary wave number, we shall write the system of linear equations expressing continuity of voltages and currents on all nodal points of the analytical scheme:

$$Z_1^{-1/2} - X_1 = X_2 - X_3 \exp(ik_C l_C),$$

$$Z_1^{1/2} + Z_1 X_1 = Z_C X_2 + Z_C X_3 \exp(ik_C l_C) + \frac{i}{\omega C_1}(Z_1^{-1/2} - X_1),$$

$$X_2 \exp(ik_C l_C) - X_3 = X_4 - X_5 \exp(ik_L l_1),$$

$$Z_C X_2 \exp(ik_C l_C) + Z_C X_3 = Z_L X_4 + Z_L X_5 \exp(ik_L l_1),$$

$$X_4 \exp(ik_L l_1) - X_5 = X_8 + X_6 - X_7 \exp(ik_L l_0),$$

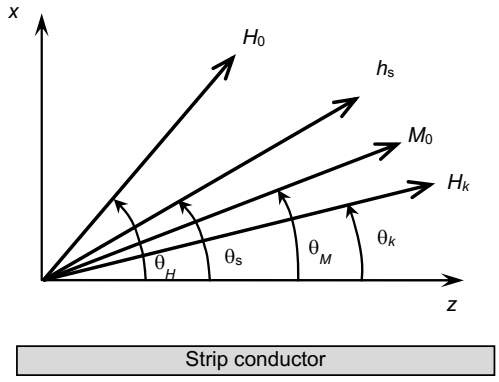

Fig. 2. Model of magnetic field with uniaxial anisotropy in the plane.

$$Z_L X_4 \exp(ik_L l_1) + Z_L X_5 = Z_L X_6 + Z_L X_7 \exp(ik_L l_0),$$

$$Z_L X_4 \exp(ik_L l_1) + Z_L X_5 = Z_2 X_8 + \frac{i}{\omega C_2} X_8, \tag{3}$$

$$Z_L X_6 \exp(ik_L l_0) + Z_L X_7 = 0,$$

where wave numbers of strip line segments are determined by expressions

$$k_C = \omega L_C C_C, \quad k_L = \omega L_L C_L, \tag{4}$$

and their characteristic impedances – by expressions

$$Z_C = \sqrt{L_C / C_C}, \quad Z_L = \sqrt{L_L / C_L}. \tag{5}$$

Numerically solving this system of linear equations, one can find all unknown currents X_j. Calculation of capacitances and inductances per unit length of microstrip transmission lines was performed in quasi-static approximation. The details of such calculation are described in [15], and its generalization for the case of presence of a ferromagnetic film with uniaxial magnetic anisotropy was done in [14]. The calculation assumed that the strip conductor of the resonator is directed along axis z, and magnetic film is in the single-domain state and magnetized at an angle θ_M to axis z (Fig. 2). We characterize uniaxial magnetic anisotropy in the film plane with anisotropy field H_k and directional angle of easy magnetization axis θ_k. The magnetic film is in the constant magnetic bias field H_0 and in the measured signal field h_s directed in the film plane at angles θ_H and θ_s to axis z respectively.

The expression determining the direction of equilibrium magnetization vector look as follows:

$$\theta_M = \operatorname{atan}\left(\frac{H_0 \sin\theta_H + h_s \sin\theta_s + H_k \cos(\theta_M - \theta_k)\sin\theta_k}{H_0 \cos\theta_H + h_s \cos\theta_s + H_k \cos(\theta_M - \theta_k)\cos\theta_k} \right). \tag{6}$$

For the examined model magnetic permeability of the film is determined by expression [14]

$$\mu_\perp = \frac{(\Omega_1 + \Omega_M)(\Omega_2 + \Omega_M) - \omega^2}{\Omega_1(\Omega_2 + \Omega_M) - \omega^2},$$

$$\Omega_1 = \gamma\left[H_0\cos\left(\theta_H - \theta_M\right) + h_s\cos\left(\theta_s - \theta_M\right) + H_k\cos 2\left(\theta_k - \theta_M\right)\right] - i\alpha\omega,$$

$$\Omega_2 = \gamma\left[H_0\cos\left(\theta_H - \theta_M\right) + h_s\cos\left(\theta_s - \theta_M\right) + H_k\cos^2\left(\theta_k - \theta_M\right)\right] - i\alpha\omega, \quad (7)$$

$$\Omega_M = \gamma 4\pi M,$$

where γ is gyromagnetic ratio, α is damping parameter, M is saturation magnetization. One should note that expressions (6) and (7) are produced by solving the Landau-Lifshitz equations [17].

For the examined microstrip design (see Fig. 1) the formula for calculation of inductance per unit length of its conductors looks as [14]

$$L = \frac{\mu_0}{\pi}\sum_{l,m=0}^{\infty} A_m^H A_l^H w_{ml}^H, \quad (8)$$

where μ_0 is magnetic permeability of vacuum, A_m^H are current expansion coefficients on the strip conductor over Chebyshev polynomials, w_{ml}^H are components of magnetic field matrix of integrals. This matrix is determined by expression

$$w_{ml}^H = (-1)^{m-l}\int_{\beta=0}^{\infty}\psi(\beta)J_{2m}\left(\frac{\beta w}{2}\right)J_{2l}\left(\frac{\beta w}{2}\right)d\beta, \quad (9)$$

where $J_m(\beta w/2)$ is the m^{th} order Bessel function of the first kind (m, l = 0, 1, 2…), w is microstrip conductor width, $\psi(\beta)$ is magnetic field function of real argument β that emerges when finding the Fourier transforms of the magnetic field vector potential at the level of strip conductors. Magnetic field function is determined by formula

$$\psi(\beta) = \frac{\sinh\left(|\beta| h_d\right)/|\beta| + C_m\cosh\left(|\beta| h_d\right)}{\left(1 + C_m|\beta|\exp(|\beta| h_d)\right)}, \quad (10)$$

where h_d is width of dielectric substrate of the thin magnetic film.

The complex parameter C_m that is part of formula (10) is the only parameter that fully describes the impact of thin magnetic film on propagation of quasi-transverse electromagnetic waves in the microstrip line [14]:

$$C_m = h_m\left[\frac{\tan\left(k_{\|} h_m\right)}{k_{\|} h_m}\sin^2\theta_M + \frac{\mu_\perp\tan\left(k_\perp h_m\right)}{k_\perp h_m}\cos^2\theta_M\right], \quad (11)$$

$$k_{\|} = \sqrt{i\omega\sigma\mu_0}, \qquad k_\perp = k_{\|}\sqrt{\mu_\perp}.$$

Here h_m is the width of magnetic film, σ is its conductivity, $k_{\|}$ and $k_\perp$ are wave vectors of waves in the film, magnetic fields of which are directed, respectively, in parallel and orthogonally to equilibrium magnetization.

At the same time, capacitance per unit length of strip segments of the microstrip structure is determined by expression

$$C = \pi\varepsilon_0 \Big/ \sum_{l,m=0}^{\infty} w_{ml}^E A_m^E A_l^E \ , \tag{12}$$

where ε_0 is dielectric permeability of vacuum, A_m^E are charge expansion coefficients on the strip conductor over Chebyshev polynomials, w_{ml}^E are components of electric field matrix of integrals.

Components of scattering matrix of the examined resonator that is a reciprocal two-port network are associated with current amplitudes X_1 and X_8 by formulas

$$\begin{aligned} S_{11} &= X_1\sqrt{Z_1}, \\ S_{21} &= X_8\sqrt{Z_2}, \end{aligned} \tag{13}$$

while $|S_{21}|^2$ is transmission coefficient or, in other words, frequency response of the examined structure. That is why value $\Delta|S_{21}|^2$ equal to the differences of values of $|S_{21}|^2$ calculated at fixed pumping frequency for two different magnetic fields of the signal h_s allows determining the sensor conversion factor K by dividing this difference by value of the measured signal h_s.

2. RESULTS OF RESEARCH ON MICROSTRIP SENSOR OF WEAK MAGNETIC FIELDS

First, let us calculate frequency response of the microstrip sensor with a thin magnetic film. In order to be able to compare the results of presented calculation with experimental results of research on the real sensor described in [13], parameters of the developed model of examined microstrip structure were taken as close to design parameters of the sensor studied in [13]. The length and width of the strip conductor of the low-impedance microstrip line segment (see Fig. 1) were $l_C = 5$ mm and $w_C = 4$ mm, substrate thickness was $h_{d1} = 0.5$ mm, its relative dielectric permeability $\varepsilon_{d1} = 80$. The length and width of the strip conductor of the high-impedance strip line segment were $l_1 = 0.4$ mm, $l_0 = 5.6$ mm, $w_L = 0.5$ mm. Permalloy film ($Ni_{75}Fe_{25}$) deposited onto the dielectric substrate with thickness $h_{d2} = 0.5$ mm and dielectric permeability $\varepsilon_{d2} = 8.5$ was selected as magnetic film. The film possesses uniaxial magnetic anisotropy and has the following parameters: saturation magnetization $M = 1100$ G, anisotropy field $H_k = 8$ Oe, damping parameter $\alpha = 0.01$, conductivity $\sigma = 2.5\cdot10^6$ Ohm$^{-1}\cdot$m^{-1} and film thickness $h_m = 0.15$ μm. Characteristic impedances of the input and output ports are $Z_1 = 50$ Ohm and $Z_2 = 10$ Ohm. As a result, calculated resonance frequency of the examined microstrip structure in the absence of magnetic film $f_0 = 0.48$ GHz coincided with resonance frequency of the sensor studied in [13] at coupling capacities at the input and at the output $C_1 = 4$ pF and $C_2 = 9.3$ pF respectively.

Fig. 3 shows normalized frequency response of the resonator built at constant magnetic bias field $H_0 = 9.6$ Oe, but for several different angles θ_H of its orientation. The axis of easy film magnetization was established as parallel to the strip conductor, i.e. $\theta_k = 0°$. One can see that maximum quality factor, just as maximum passing of microwave frequency power on resonance frequency, is observed at $\theta_H = 90°$, when there is no interaction of magnetic moment of the film with high-frequency pumping field, as far as in this case they are oriented in parallel to one another. When magnetic moment is orthogonal to the direction of pumping field $\theta_H = 0°$ (curve *4*), one observes maximum decrease in resonance frequency at the expense of increase in magnetic permeability of the film, but quality factor of the resonator remains relatively high. The largest decrease in quality factor is observed at $\theta_H = 85°$, when losses associated with ferromagnetic resonance in the film manifest themselves.

To determine the conversion factor of the examined sensor, let us direct magnetic field of the signal h_s along the conductor ($\theta_s = 0°$). Fig. 4 presents the dependence of maximally normalized conversion factor upon the constant magnetic bias field H_0 applied at the angle $\theta_H = 90.5°$. One can see that position of the conversion factor maximum corresponds to the field of film anisotropy $H_k = 8$ Oe, and this agrees well with the fact experimentally established in [13]. It is important to note [13] that to reduce the noises in the real sensor, displacement magnetic field ought to be larger than anisotropy field by approximately 20%.

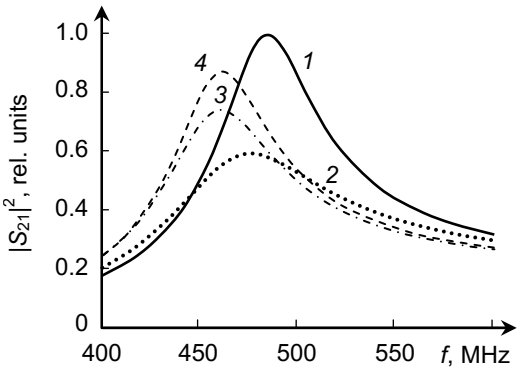

Fig. 3. Frequency response of the microstrip sensor for different orientation angles of magnetic bias field $H_0 = 9.6$ Oe: $\theta_H = 90°$ (curve *1*), 85° – (curve *2*), 70° (curve *3*), 0° (curve *4*).

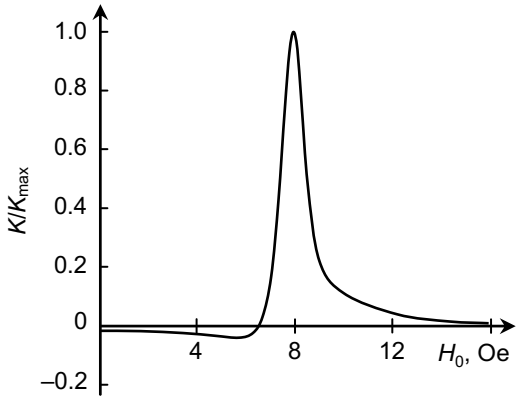

Fig. 4. Dependence of conversion factor on the value of magnetic bias field H_0 for $\theta_H = 90.5°$.

Behavior of frequency response presented on Fig. 3 allows suggesting that under the impact of the measured magnetic field h_s a change in magnetic permeability of the thin film leads to simultaneous resonance frequency shift and change in quality factor of the resonator. That is why the sensor conversion factor will considerably depend on the chosen pumping frequency.

Fig. 5 (curve *1*) presents the dependence of maximally normalized sensor conversion factor K/K_{max} built from the directional angle of magnetic bias field θ_H, at its value $H_0 = 10$ Oe and pumping frequency $f = 510$ MHz. One can see that there are two pronounced extreme points on the dependence at certain directional angles of the magnetic bias field. This result agrees well with the measurement results for the microstrip sensor of weak magnetic fields presented in [13].

It is well-known that in magnetic films one always observes heterogeneities of magnetic characteristics throughout their area, associated with heterogeneities of the substrate surface and technological characteristics of the film production process [18, 19]. The calculation presented in the paper allows carrying out research on the impact of heterogeneities of magnetic parameters of the film on the microstrip characteristics. For instance, research was done on the impact of amplitude and angular dispersion of uniaxial magnetic anisotropy field characterized by normal law of distribution upon the sensor conversion factor. As expected, with the rise in amplitude and angular dispersion of anisotropy field, the sensor conversion factor monotonously decreases. Moreover, angular dispersion has a stronger impact on K. Increase in angular dispersion of anisotropy $\delta\theta_k$ from zero to 1° reduces the maximum value of conversion

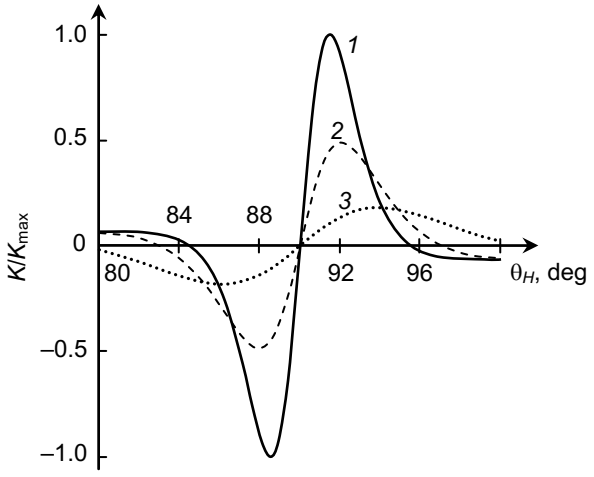

Fig. 5. Dependences of normalized conversion factors of the microstrip sensor from the directional angle of magnetic bias field built at $H_0 = 10$ Oe for different values of angular dispersion of uniaxial magnetic anisotropy $\delta\theta_k$: curve *1* – 0°, curve *2* – 2°, curve *3* – 5°.

factor more than twofold (Fig. 5), and at $\delta\theta_k = 5°$ conversion factor decreases more than five times. We note that amplitude dispersion of uniaxial magnetic anisotropy of relatively large value $\delta H_k = 2$ Oe leads to decrease in conversion factor by less than 20%.

CONCLUSIONS

The authors developed a one-dimensional model of a miniature sensor of weak magnetic fields on the microstrip structure with a thin magnetic film that offers a possibility to produce in quasi-static approximation the necessary formulas for numerical calculation of the considered design. In theory, the calculation allows carrying out research on the impact of various design parameters of the sensor, including magnetic field parameters, upon the device characteristics. Taking into account the large number of microstrip structure and magnetic film parameters affecting the sensor characteristics, such studies are necessary for optimization of its design, in order to reach the maximum possible characteristics.

What proves the validity of using quasi-static approximation when calculating the numerical model of the sensor is, first, the concurrence of resonance frequency of the examined design with the measured resonance frequency on experimental sample with identical design parameters [13]. Second, the calculated dependence of conversion factor of the sensor built from the direction angle of constant magnetic bias field shows two strongly pronounced extreme points at certain angles, which also conforms well with the measurement results presented in [13]. And finally, the fact experimentally established in [13] that the maximum conversion factor is observed in magnetic bias field close to the field of uniaxial magnetic anisotropy is confirmed theoretically in the present paper.

Theoretical calculation allowed examining the impact of angular and amplitude dispersion of uniaxial magnetic anisotropy of the thin film characterized by normal law of distribution on the sensor characteristics. It was shown that with the rise in amplitude and angular dispersion of the anisotropy field the sensor conversion factor decreases monotonously. Moreover, angular dispersion has a stronger effect on K. Increase in angular dispersion of anisotropy $\delta\theta_k$ from zero to 1° reduces the maximum value of conversion factor more than twofold (Fig. 5), while at $\delta\theta_k = 5°$ conversion factor decreases more than five times. Amplitude dispersion of uniaxial magnetic anisotropy of comparatively large value $\delta H_k = 2$ Oe leads to decrease in the conversion factor by less than 20%.

This research was performed with support of the Russian Ministry of Education and Science, project No. RFMEFI60417X0179.

REFERENCES

1. K. Erkan and C. Jekeli, J. Appl. Geophys., **74**, 142–150 (2011).
2. D. Gubbins, Space Sci. Rev., **155**, 9–27 (2010).
3. H. U. Auster, K. H. Glassmeier, W. Magnes, and O. Aydogar, Space Sci. Rev., **141**, 235–264 (2008).
4. M. Díaz-Michelena, Sensors, **9**, 2271–2288 (2009).
5. C. Gaffney, Archaeometry, **50**, Issue 2, 313–336 (2008).
6. T. Wang, Y. Zhou, C. Lei, and J. Luo, Biosens. Bioelectron., **90**, 418–435 (2017).
7. A. Grosz, M. J. Haji-Sheikh, and S. C. Mukhopadhyay, High Sensitivity Magnetometers, Switzerland, Springer (2017).
8. A. E. Mahdia, L. Panina, and D. Mapps, Sensors and Actuators A., **105**, 271–285 (2003).
9. D. Budker and M. Romalis, Nature Phys., **3**, 227–234 (2007).
10. E. B. Aleksandrov and A. K. Vershovskii, Physics-Uspekhi, **52**, Issue 6, 573–602 (2009).
11. P. Ripka, Sensors and Actuators A., **33**, 129–141 (1992).
12. J. E. Danielsena, E. Auken, F. Jorgensen, *et al*., J. Appl. Geophys., **53**, 181–198 (2003).
13. A. N. Babitskii, B. A. Belyaev, N. M. Boev, *et al*., Instruments and Experimental Techniques, **59**, Issue 3, 425–432 (2016).
14. V. V. Tyurnev, Journal of Communications Technology and Electronics, **53**, Issue 7, 814–822 (2008).
15. V. V. Tyurnev, Microwave Circuit Theory [in Russian], Krasnoyarsk, KSTU publishing center (2003).
16. K.C. Gupta, R. Garg, R. Chadha, Computer-Aided Design of Microwave Circuits, Artech House (1981).
17. A. G. Gurevich, Magnetic Resonance in Ferrite and Antiferromagnetic Materials [in Russian], Nauka, Moscow (1973).
18. B. A. Belyaev, A. V. Izotov, S. Ya. Kiparisov, G. V. Skomorokhov, Physics of the Solid State, **50**, Issue 4, 676–683 (2008).
19. B. A. Belyaev, A. V. Izotov, and P. N. Solovev, Physica B., **481**, 86–90 (2016).